View metadata, citation and similar papers at core.ac.uk

brought to you by CORE

provided by eScholarship@BC

All-angle negative refraction of photonic and polaritonic waves in three-dimensionally periodic structures

Author: Alec Daniel Rose

Persistent link: http://hdl.handle.net/2345/685

This work is posted on eScholarship@BC,
Boston College University Libraries.

Boston College Electronic Thesis or Dissertation, 2009

Copyright is held by the author, with all rights reserved, unless otherwise noted.

Boston College

College of Arts and Sciences Honors Program

Physics Department

ALL-ANGLE NEGATIVE REFRACTION OF PHOTONIC AND POLARITONIC WAVES IN THREE-DIMENSIONALLY PERIODIC STRUCTURES

By
ALEC ROSE

May 1, 2009

Advisor: Dr. Krzysztof Kempa

Abstract

Though nature provides a plethora of materials to work with, their properties are very much restricted, forcing severe limitations on the devices that are built from them. A huge portion of current technology stands to be significantly advanced and even revolutionized by the emergence of a new class of "configurable" materials. This class, generally referred to as metamaterials, has become more feasible than ever due to advancements in nanotechnology and fabrication techniques. Notable among nature's limitations is an ever-positive index of refraction. This barrier has only recently been broken, and the known paths to negative refraction are few and limited. This paper introduces two distinct three-dimensional crystals capable of all-angle negative refraction. One uses the familiar photonic band, while the other is the first of its kind to rely on polaritonic waves. Their mode structures are examined and a set of parameters are chosen at which a negative effective index of refraction can be harnessed for unrestricted sub-wavelength lensing, demonstrated via numerical simulation. This work is expected to enable experimental observation of polaritonic negative refraction and sub-wavelength lensing at microwave frequencies.

Key Words: photonic, polaritonic, metamaterial, negative refraction, super or sub-wavelength lens, point-dipole

Table of Contents

1. Introduction

While negative refraction was initially proposed by Veselago in the 1960's [1], it has recently attracted strong research interests [2-14], since negatively refractive materials can now be realized with nanotechnology. The most exciting consequence of this is the possibility of sub-wavelength lensing [13]. A slab made of a material with an isotropic refractive index $n = -1$ restores not only phases of the transmitted propagating waves, but also amplitudes of the evanescent waves that are responsible for the sub-wavelength details of the source geometry [13]. Such a material (metamaterial) can be used to make a superlens capable of exceeding the diffraction limit of conventional lenses. The applications of such a lens are quite broad, ranging from nanolithography to microscopy and detection. This method of imaging, however, does have its own limitations due to the inherent losses in the media, which have been investigated in references 15 and 16.

Various approaches were used to demonstrate these exotic properties. In one instance, negative refraction was achieved in a system consisting of split-ring resonators and metal wires [3-5]. In another approach, it was shown that a dielectric, three-dimensional (3D) photonic crystal (PC) can act as a metamaterial with an effective negative refractive index [17]. More recently, two-dimensional (2D) polaritonic crystals based on a point-dipole system have been explored as a possible route to superlensing [22]. This paper extends the polaritonic superlens to three dimensions, proposes a new 3D photonic superlens, and outlines possible fabrication methods for both systems. All results and figures introduced in this work were created via a combination of finite

difference time domain and frequency domain (FDTD and FDFD) computational schemes [20].

2. Point-Dipole Crystal

The method of using a polaritonic crystal to achieve negative refraction began with a 3D cubic crystal of point-dipoles. It was shown that the system is a non-local polaritonic crystal that allows for bulk and surface plasmon wave propagation, in addition to the bands, gaps, and other effects generally found in PCs [23]. On top of this, the right choice of parameters allows for negative refraction and sub-wavelength lensing over a specific frequency range.

In one approach, a very thin film (with thickness << λ) of a crystal made of Ag nanoparticles was proposed to emulate the point-dipole crystal. It was shown to exhibit negative refraction in similar fashion to a thin Ag film, but with less efficiency [13,24]. Subsequently [23], a thick film of the point-dipole crystal was considered with each dipole assumed to have the following equation for polarization

$$\alpha(\omega) = \frac{\omega_p^2}{4\pi(\omega_0^2 - \omega^2)} = \frac{\Omega_p^2}{4\pi(\Omega_0^2 - \Omega^2)} \qquad (1)$$

where $\Omega = \omega a/c$ is a normalized frequency, and $\Omega_0 = \omega_0 a/c$ and $\Omega_p = \omega_p a/c$ are the variable parameters. The constants involved are *a*, the lattice constant; *c,* the speed of light; ω_0, the resonance frequency of the charges; and ω_p, a constant with dimensions of frequency. Next, the parameters were adjusted so that the mode structure acquired the

form as shown in Fig. 1. The inset clarifies the topology of the bands, illustrating the minimum-bending avoided-crossing of the photon line with the longitudinal polarization (LP) and transverse polarization (TP) asymptotics. The left and right panels show the cases before and after the mode interaction has been "switched on," respectively. The Brillouin zone has been specifically adjusted so that the photon line is "Umklapped" before crossing the asymptotics. This results in both upper bands acquiring a negative slope, and therefore negative refraction is expected at the frequency given by the intersection of the vacuum light line with these branches. This system's negative refraction is thus mediated by polaritonic waves rather than by the pure TEM modes, which is generally the case in PCs.

3. 3D Polaritonic Crystal

In order to verify the occurrence of negative refraction and sub-wavelength lensing in a realistic dipole-like crystal, we chose a face centered cubic (FCC) lattice of spheres (radius r) with high dielectric constant (ε_s) embedded in a low dielectric medium (ε_b). We let ε_b=1 (air), ε_s=30, and r =.31a, where a is the conventional lattice constant of a cubic FCC cell. This set of parameters corresponds to the band structure shown in Fig. 2. The high contrast in dielectric materials assures that the individual sphere response is essentially dipolar, while the radius was chosen such that it maximized the negative slope of the band of interest. The FCC lattice is preferable to a simple cubic lattice due its greater isotropy, a necessary component of all-angle negative refraction (AANR). The increase in isotropy helps specifically in the construction of a spherical equifrequency surface (EFS), which is the mode surface created in k-space by assuming a constant

frequency, much like the Fermi-surface in electronics. The EFS necessary for negative refraction in this crystal can be seen in the area around the Γ point of the band structure. Again, the point of interest is the intersection of the vacuum light line with the negatively sloped, polaritonic band. At this normalized frequency, Ω = 2.14, it was found that AANR does indeed occur.

Subsequently, we investigated the sub-wavelength lensing properties of a slab (width *w*) of this material using a line-source placed a distance *d* from the slab-air interface. For a metamaterial with an effective index of refraction *n* = -1, the image center is expected to exist on the opposing side of the crystal at a distance $x = w - d$. Fig. 3 demonstrates the superlensing capabilities of a slab of this crystal. The image is clearly visible at the expected position, indicating that the slab is indeed functioning as a metamaterial with $n = -1$. Additionally, the image location follows the expected geometric rules of optics for different source positions and slab thicknesses, as demonstrated in Fig. 4, thus verifying that the superlensing is unrestricted. This is the most important step of testing a superlens, as restricted lensing, or "channeling," severely limits the applicability of the material [18]. However, the image quality depends strongly on the slab's edges and orientation. The configuration displayed here, in which the "cuts" were made along the Γ-X direction and directly through the sphere centers, was found to achieve the highest efficiency and resolution for this particular choice of parameters. Thus, the major limitation to resolution is most likely the complex surface effects, which are ignored in a mode structure analysis. This limitation aside, additional improvements to resolution can be achieved by employing a more complex basis [21].

4. 3D Photonic Crystal

The FCC lattice of spheres also lends itself to the construction of a PC. Thus, we consider a second crystal with air spheres suspended in a dielectric matrix. Since this system is more or less the inverse of the previous system, it cannot be considered dipole-like, and it is therefore strictly a PC, capable of all the properties found in such materials [19]. The parameters are chosen to be $\varepsilon_s = 1$, $\varepsilon_b = 30$, and r = .32a, with a corresponding band diagram in Fig. 5. The most spherical EFS's exist at a frequency of $\Omega = 2.26$. However, the band diagram shows that this frequency supports multiple modes. While this seems problematic, it turns out that as long as the bands have very similar slopes and positions, an effective refractive index can still be defined for the material. Additionally, the blue bands (whose slopes and positions are not similar) can be ignored as their wave vectors at the frequency of interest are too far from that of vacuum light for efficient coupling in the presence of the other, better-matched modes.

The superlensing results are displayed in Fig. 6 and 7. Once again, a quality image is recovered at the expected position, demonstrating that this crystal slab is also an unrestricted superlens. However, it is worth noting that this system is less dependent on slab termination than the previous one, and a recognizable image is recovered for all terminations along the Γ-X axis, as long as the crystal symmetry is preserved. This is most likely due to the presence of multiple bands at the frequency of interest. For any given termination, the incoming waves are able to couple to at least one of these modes within the slab, while the previous system was restricted to a single mode. Again, the systems presented here are the most efficient of the scenarios that we attempted, corresponding to a cut through the centers of the spheres. Additionally, the resolution of

these images is improved over those for the polaritonic crystal. This again can be attributed to the surface effects, which are apparently more isotropic and less damaging in the PC. Further investigation should lead to a surface design that minimizes these effects in both crystals, maximizing the resolution.

5. Fabrication Proposal

Both of these crystals should be quite feasible in the microwave range. Commercially available polymer-ceramic composites can satisfy the required dielectric constant of 30 for each system. Letting a = 1 cm, the polaritonic crystal could easily be constructed from a network of polymer-ceramic spheres of radius .31cm, held in place by something as simple as thread running through the center of each sphere. The radiation vacuum wavelength of interest for this system is 2.94 cm, corresponding to a frequency of 10.2 GHz. The PC superlens, on the other hand, would require low index spheres of radius .32cm submerged in a block of the polymer-ceramic composite. This low index material could range from Styrofoam to low-index glass, though care must be taken when choosing this material as it is the large ratio in dielectric constant that gives the system its specific band structure. The frequency at which negative refraction should be expected in the PC is 10.8 GHz. Appropriate slabs of these proposed materials should allow for observable 3D sub-wavelength lensing in the microwave range, and while this has been achieved previously via PCs, it has yet to be demonstrated in a polaritonic crystal.

6. Conclusions.

Metamaterials appear poised to bridge the gaps that nature by itself cannot fill, as evidenced by the recent studies involving negative refraction and subwavelength lensing in photonic and polaritonic crystals. In particular, the 3D polaritonic crystal of point dipoles proposed in reference 23 was shown to exhibit many interesting optical effects, including photonic and polaritonic band gap formation, plasma waves, and negative polaritonic refraction. In this work, we propose a practical realization of such a system: the dipole-like, FCC crystal of dielectric spheres. The electromagnetic response of these spheres is shown to emulate the point-dipoles to a high degree, and unrestricted sub-wavelength lensing can be expected from such a material. Meanwhile, the PC inverse of this system is likewise predicted to exhibit AANR and sub-wavelength lensing. The proposed systems are easy to fabricate, and the negative refraction is designed to occur in the highly accessible microwave range. An experimental attempt to complement these results is strongly encouraged.

Acknowledgements

This work was supported in part by the Polish Ministry of Higher Education (Ministerstwo Nauki i Szkolnictwa Wyzszego) through the grant 3940/T02/2007

References

1. V. G. Veselago, Sov. Phys. Ups. **10**, 509 (1968).
2. H. Kosaka, T. Kawashima, A. Tomita, M. Notomi, T. Tamamura, T. Sato, and S. Kawakami, Phys. Rev. B **58**, 10 096 (1998).
3. J.B. Pendry, A.J. Holden, W.J. Stewart, and I. Youngs, Phys. Rev. Lett. 76, 4773 (1996).
4. J.B. Pendry, A.J. Holden, D.J. Robbins, and W.J. Stewart, IEEE Trans. Microwave Theory Tech. 47, 2075 (1999).
5. D.R. Smith, W.J. Padilla, D.C. Vier, S.C. Nemat-Nasser, and S. Schultz, Phys. Rev. Lett. **84**, 4184 (2000).
6. D.R. Smith and N. Kroll, Phys. Rev. Lett. 85, 2933 (2000).
7. R.A. Shelby, D.R. Smith, S.C. Nemat-Nasser, and S. Schultz, Appl. Phys. Lett. **78**, 489 (2001).
8. R.A. Shelby, D.R. Smith, and S. Schultz, Science **292**, 77 (2001).
9. R.W. Ziolkowski and E. Heyman, Phys. Rev. E **64**, 056625 (2001).
10. M. Bayindir, K. Aydin, E. Ozbay, P. Markos, and C.M. Soukoulis, Appl. Phys. Lett. **81**, 120 (2002).
11. R.M. Walser, A.P. Valanju, and P.M. Valanju, Phys. Rev. Lett. **87**, 119701 (2001).
12. D.R. Smith, D. Schurig, and J.B. Pendry, Appl. Phys. Lett. **81**, 2713 (2002).
13. J. B. Pendry, Phys. Rev. Lett. **85**, 3966 (2000).

14. P.V. Parimi, W.T. Lu, P. Vodo, J. Sokoloff, J.S. Derov and S. Sridhar, Phys. Rev. Lett. 92, 127401 (2004).

15. R. Merlin, Appl. Phys. Lett. 84, 1290 (2004).

16. D. R. Smith, D. Schurig, M. Rosenbluth, S. Schultz, S. A. Ramakrishna and J. B. Pendry, Appl. Phys. Lett. 82, 1506 (2003).

17. C. Luo, S.G. Johnson, and J.D. Joannopoulos, Appl. Phys. Lett. 81, 2352 (2002).

18. X. Wang, Z. F. Ren, and K. Kempa, Opt. Express 12, 2919-2924 (2004), http://www.opticsexpress.org/abstract.cfm?URI=OPEX-12-13-2919.

19. J. D. Joannopoulos, R. D. Meade, and J. N. Winn, *Photonic Crystals: Molding the Flow of Light* (Princeton University Press, Princeton, 1995).

20. A.Taflove, Computational Electrodynamics—The Finite-Difference Time-Domain Method (Artech House, Norwood, MA, 1995).

21. X. Wang and K. Kempa, Applied Physics Letters 86, 061105 (2005).

22. X. Wang and K. Kempa, Phys. Rev. B 71, 233101 (2005).

23. K. Kempa, R. Ruppin, and J. B. Pendry, Phys. Rev. B 72, 205103 (2005);

24. R. Ruppin, J. Phys.: Condens. Matter **17**, 1803 (2005);

Figures

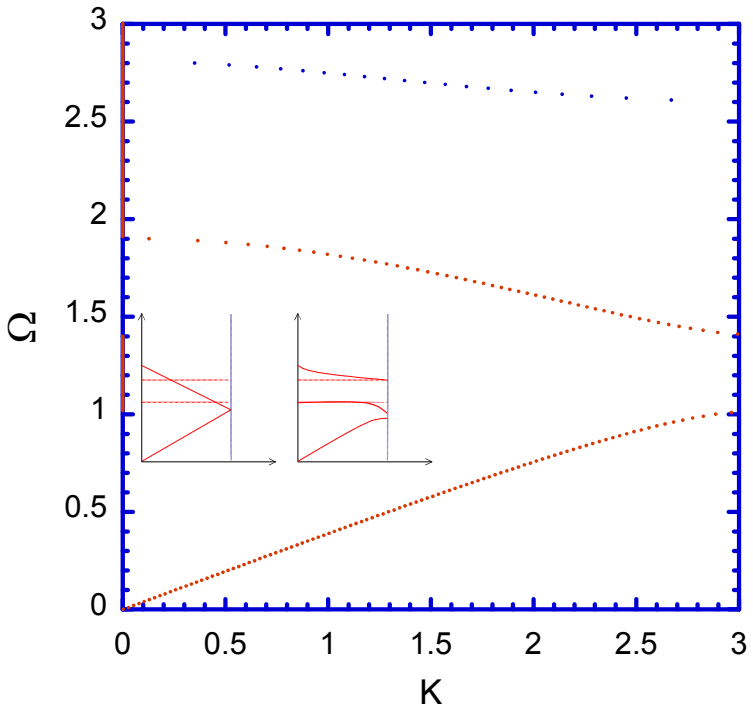

Fig. 1 Band structure of a point dipole crystal with $\Omega_0 = \Omega_p = 3$, and $\varepsilon_b = 5$. The inset shows a schematic of the light line anti-crossing with the dipolar modes (the horizontal TP and LP, corresponding to the dashed lines). The normalized wave vector is $K = ka$ (taken form Ref. 23).

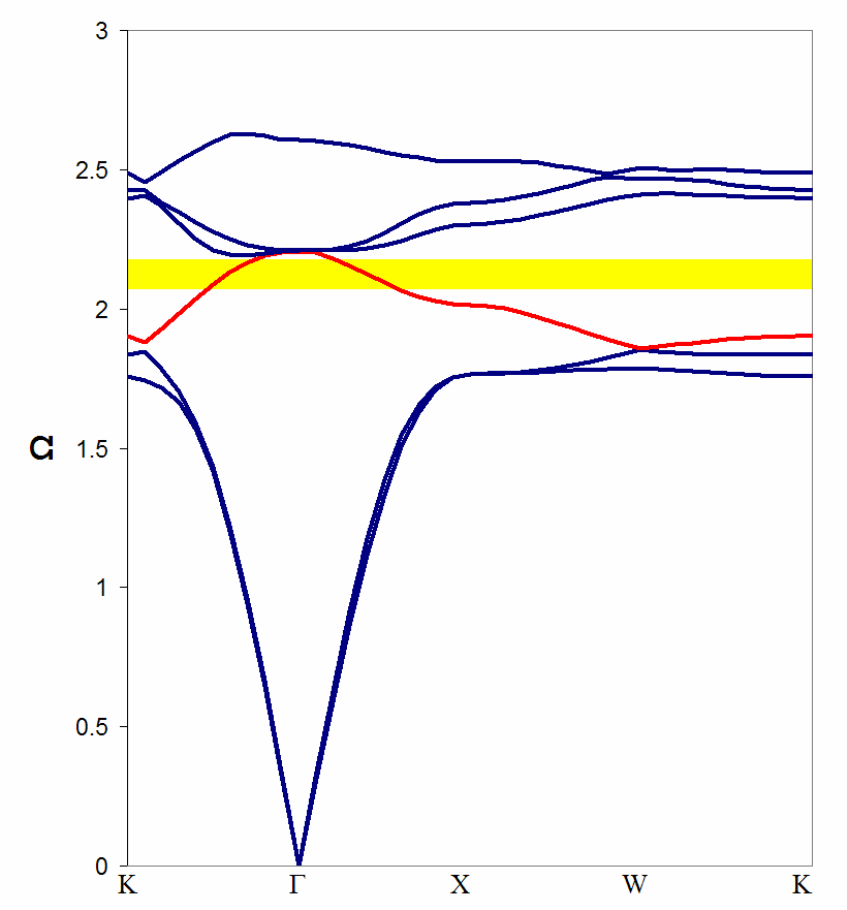

Fig. 2 Band diagram for an FCC lattice of dielectric spheres (dipole-like polaritonic crystal) with $\varepsilon_b = 1$, $\varepsilon_s = 30$, and $r = .31a$. The major symmetry points are labeled along the lower axis. The portion of the red band that falls within the yellow region indicates where AANR is expected. Compare the Γ-X portion of this plot to Fig. 1.

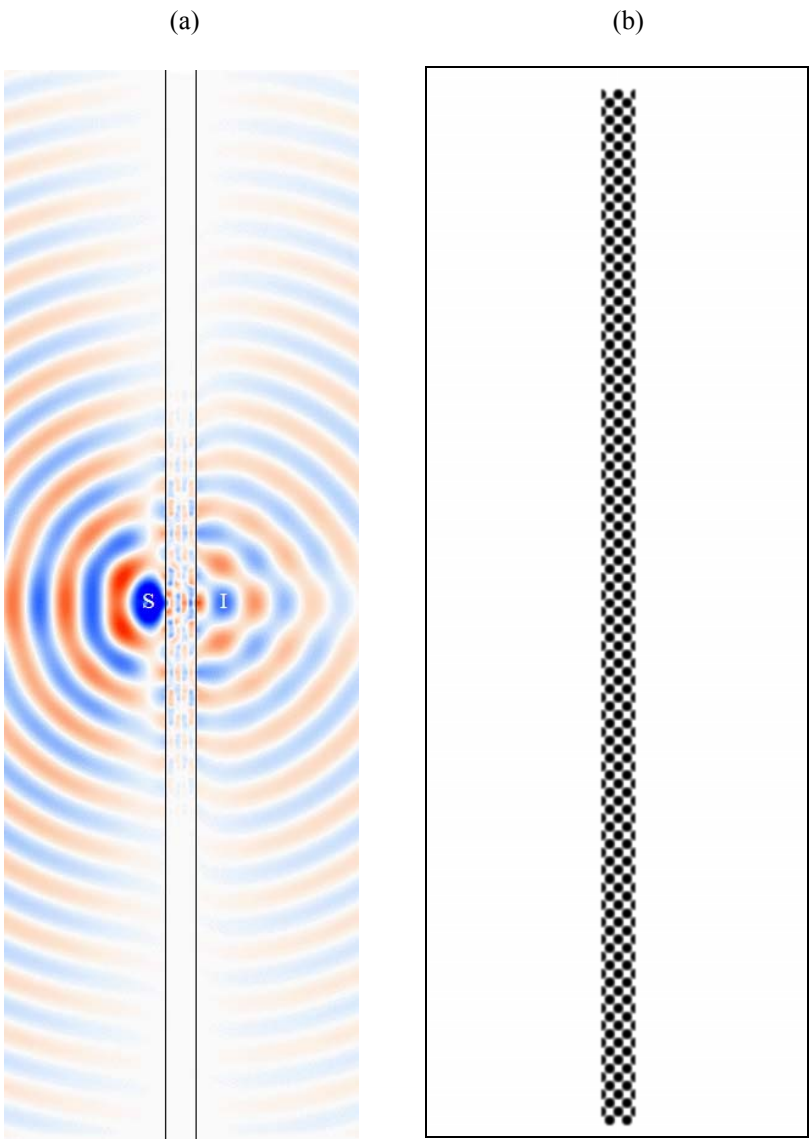

Fig. 3 (a) The propagation map (color coded electric field distribution across space, where the fields shown are perpendicular to the plane of the page) for a slab of the 3D polaritonic crystal acting as a superlens, with $w = 2a$ and $d = a$. Color intensity signifies field strength, while red denotes positive and blue denotes negative values. The labels 'S' and 'I' mark the centers of the source and image, respectively. (b) The corresponding dielectric composition of the slab.

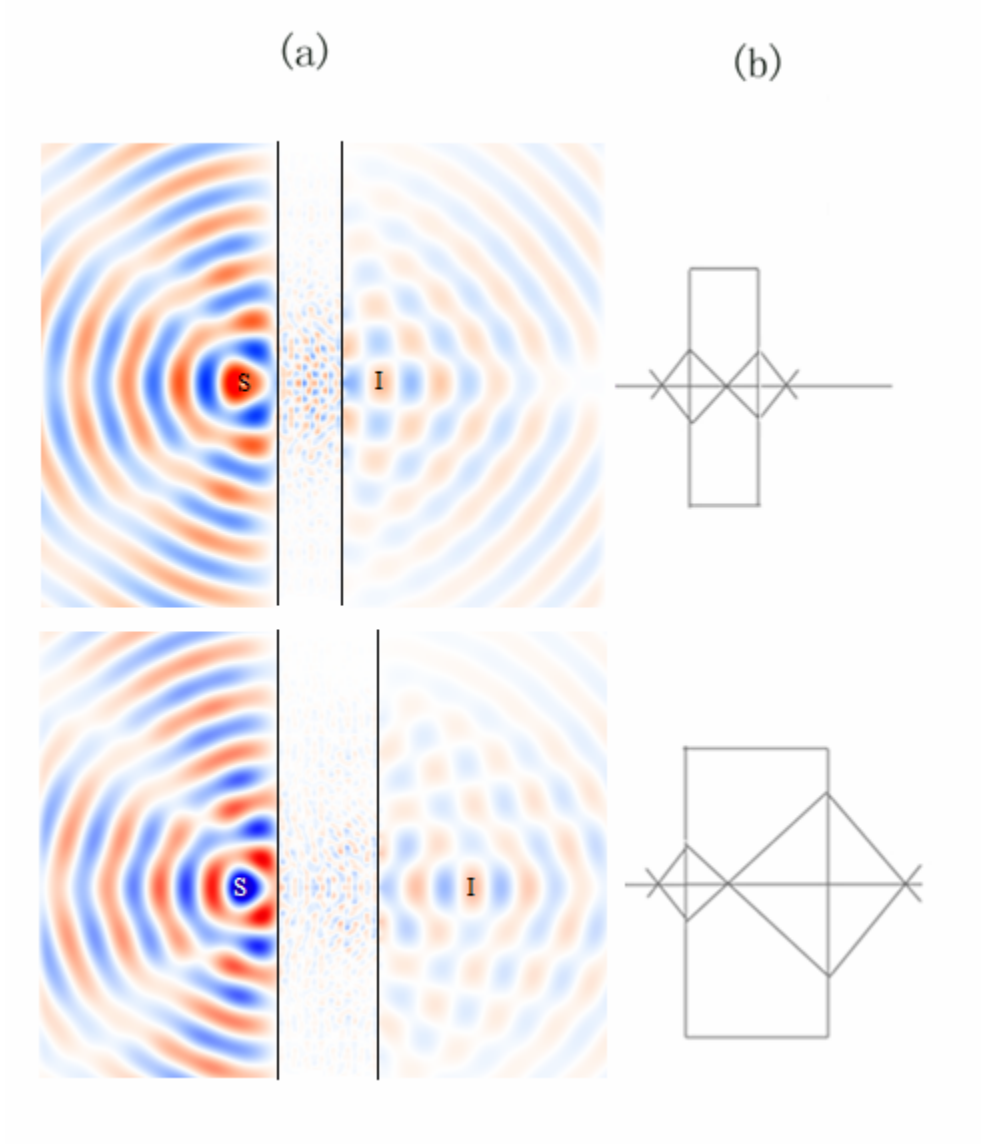

Fig. 4 (a) The propagation maps for two slabs of the 3D polaritonic crystal. (b) The corresponding sketches of the geometric optics analysis (Snell's Law) for an effective medium with $n=-1$, showing that for a thicker slab (lower panel) the image must be further away from the crystal edge. The locations of the images show great agreement with this analysis, implying unrestricted superlensing and AANR.

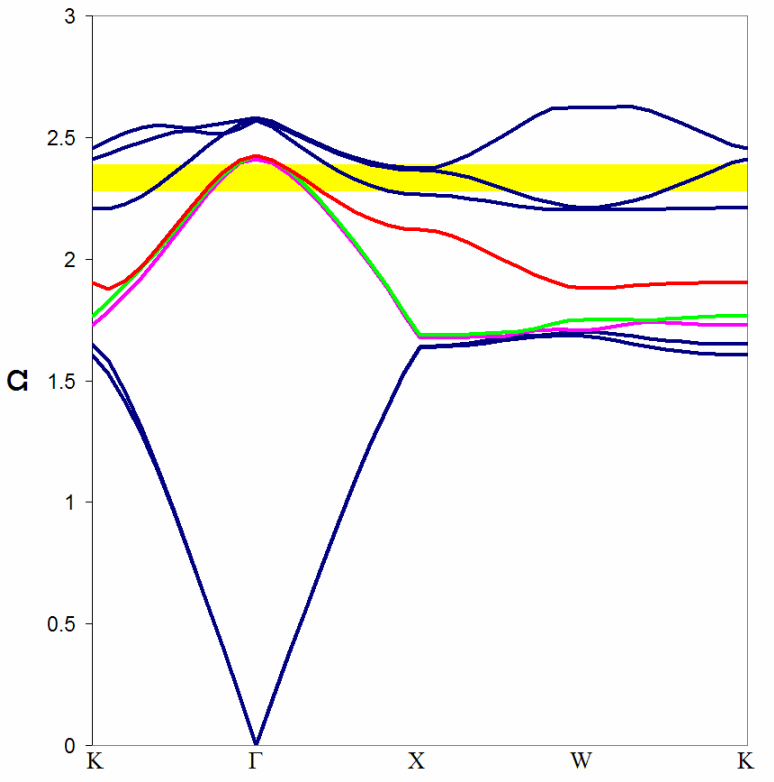

Fig. 5 The band structure for an FCC lattice of air spheres suspended in a dielectric medium (photonic crystal) with $\varepsilon_b = 30$, $\varepsilon_s = 1$, and r = .32a. The major symmetry points are labeled along the lower axis. The portions of the red, green, and pink bands that fall within the yellow region indicate where AANR is expected.

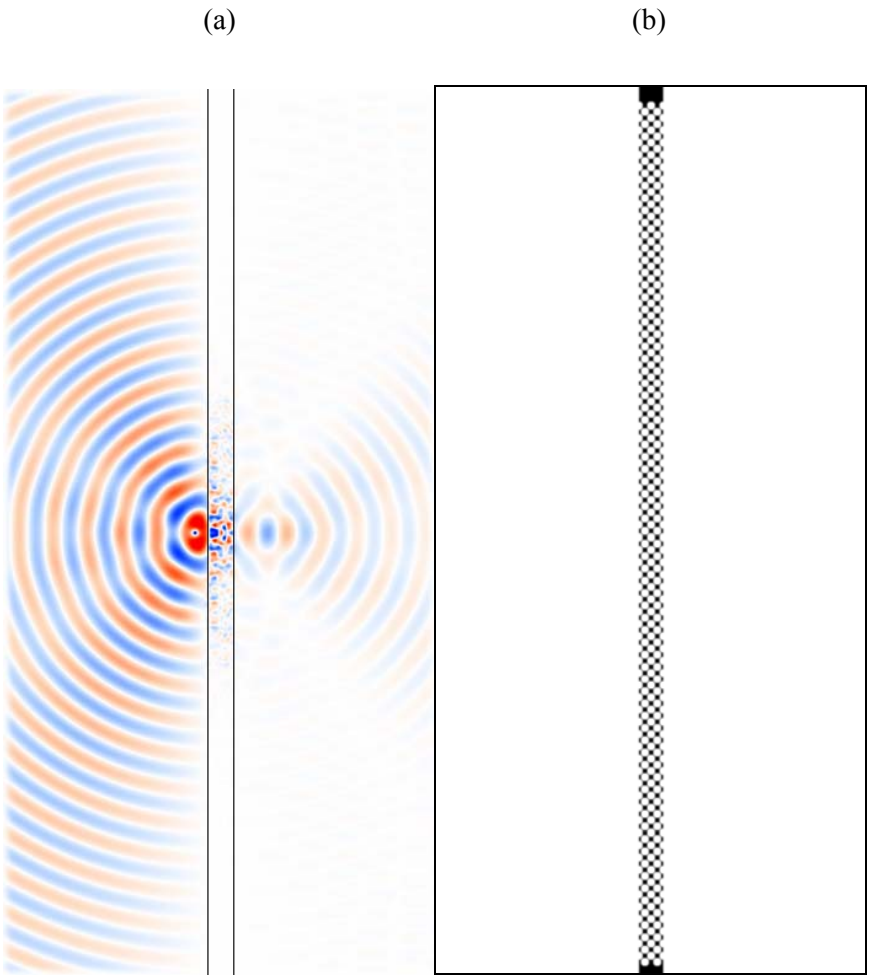

Fig. 6 (a) The propagation map for a slab of the 3D photonic crystal acting as a superlens. (b) The corresponding dielectric composition of the slab.

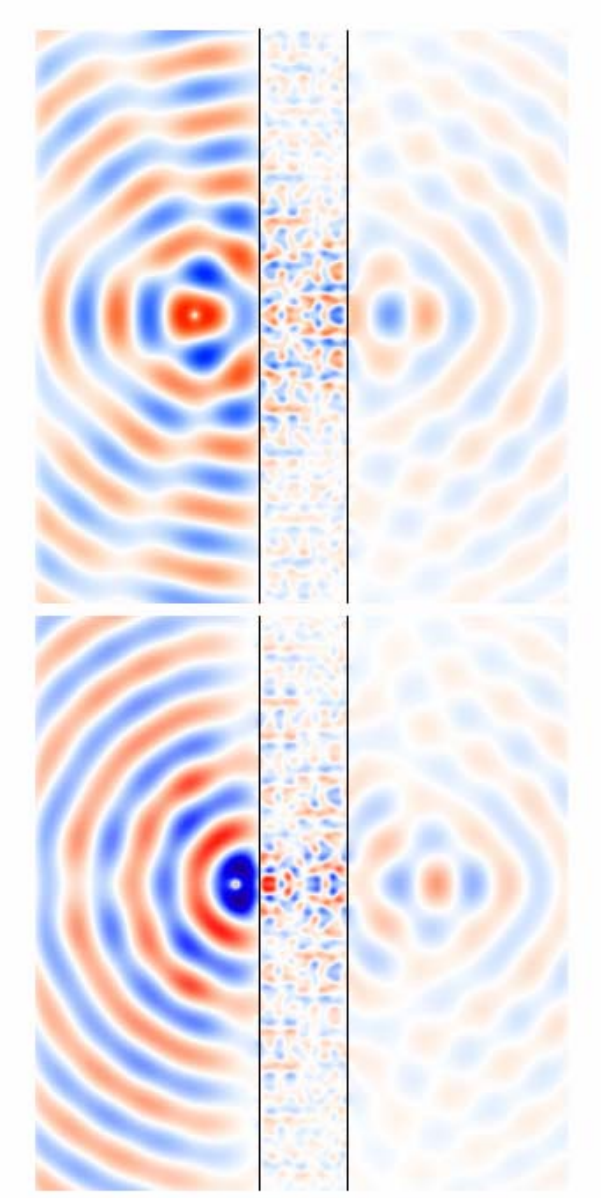

Fig. 7 The propagation maps for a slab of the 3D PC for varying source positions. The locations of the images agree with the geometric optics analysis where the PC is considered an effective medium with $n = -1$ and a Snell's Law refraction is assumed to occur at each interface, giving a predicted image distance of $x = w - d$.